

A doxycycline inducible, adenoviral bone morphogenetic protein-2 gene delivery system to bone

Jennifer J. Bara¹, Iska Dresing¹, Stephan Zeiter¹, Martina Anton², Guy Daculsi³, David Eglin¹, Dirk Nehrbass¹, Vincent A. Stadelmann¹, Duncan C. Betts⁴, Ralph Müller⁴, Mauro Alini¹ and Martin J. Stoddart^{1*}

¹AO Research Institute Davos, Davos Platz, Switzerland

²Klinikum Rechts der Isar der Technischen Universität München, Institute of Experimental Oncology and Therapy Research, Munich, Germany

³INSERM U791 Laboratory for Osteoarticular and Dental Tissue Engineering, Dental Faculty, Nantes University, Nantes, France

⁴Institute for Biomechanics, ETH Zurich, Zurich, Switzerland

Abstract

We report the novel use of a tuneable, non-integrating viral gene delivery system to bone that can be combined with clinically approved biomaterials in an 'off-the-shelf' manner. Specifically, a doxycycline inducible Tet-on adenoviral vector (AdTetBMP-2) in combination with mesenchymal stromal cells (MSCs), fibrin and a biphasic calcium phosphate ceramic (MBCP®) was used to repair large bone defects in nude rats. Bone morphogenetic protein-2 (BMP-2) transgene expression could be effectively tuned by modification of the doxycycline concentration. The effect of adenoviral BMP-2 gene delivery upon bone healing was investigated *in vivo* in 4 mm critically sized, internally fixated, femoral defects. MSCs were transduced either by direct application of AdTetBMP-2 or by pre-coating MBCP granules with the virus. Radiological assessment scores post-mortem were significantly improved upon delivery of AdTetBMP-2. In AdTetBMP-2 groups, histological analysis revealed significantly more newly formed bone at the defect site compared with controls. Newly formed bone was vascularized and fully integrated with nascent tissue and implanted biomaterial. Improvement in healing outcome was achieved using both methods of vector delivery (direct application vs. pre-coating MBCP). Adenoviral delivery of BMP-2 enhanced bone regeneration achieved by the transplantation of MSCs, fibrin and MBCP *in vivo*. Importantly, our *in vitro* and *in vivo* data suggest that this can be achieved with relatively low (ng/ml) levels of the growth factor. Our model and novel gene delivery system may provide a powerful standardized tool for the optimization of growth factor delivery and release for the healing of large bone defects. Copyright © 2016 John Wiley & Sons, Ltd.

Received 25 April 2016; Revised 6 September 2016; Accepted 6 December 2016

Keywords gene delivery; BMP-2; biomaterial; tissue engineering; mesenchymal stromal cell; bone repair

Introduction

Bone defects and non-union fractures resulting from trauma, tumour resection or other skeletal abnormalities represent a major clinical problem in orthopaedic medicine. Clinical interventions for large bone defects and non-union fractures include autologous or allogeneic bone grafting, but limitations in supply result in difficulties for the repair of large or multiple defects – a problem that is exacerbated by our aging population. Moreover, a good clinical outcome is not always achieved and allogeneic tissue transplantation is associated with risks of disease transmission and immunological complications (Burchardt, 1987; Goel *et al.*, 2005). Although routinely used in dental practice, xenograft bone substitutes are less favoured for large bone defect repair in orthopaedics due to volume requirements and the association with post-surgical complications. Ceramic biomaterials offer a synthetic alternative to bone graft,

exhibiting potent osteoinductive properties *in vivo* (Barradas *et al.*, 2011). Micro-macroporous biphasic calcium phosphate (MBCP®) hydroxyapatite ceramic has been studied extensively in animal models of bone repair (Goyenvalle *et al.*, 2010; Jegoux *et al.*, 2005; Le Nihouannen *et al.*, 2008; Saffarzadeh *et al.*, 2009) and more recently has demonstrated safety and clinical efficacy in the treatment of tooth extractions (Weiss *et al.*, 2007) and benign bone tumours and lesions (Reppenhagen *et al.*, 2012).

Mesenchymal stromal cells (MSCs) have been extensively studied as a cell-source for bone regeneration and are thought to contribute to healing by direct cellular differentiation, paracrine activity and immunomodulation. *In vitro* expanded MSCs have demonstrated therapeutic efficacy when used for the treatment of osteogenesis imperfecta (Horwitz *et al.*, 2002), bone defects (Marcacci *et al.*, 2007) and non-union fractures in man (Quarto *et al.*, 2001). However, complete functional regeneration of large bone defects or non-union fractures has not been achieved using MSCs or biomaterials alone. Cell-based therapies, biomaterial implantation and drug/gene therapy used alone or in combination are considered to be the future of biological

*Correspondence to: Martin J. Stoddart, AO Research Institute Davos, Clavadelstrasse 8, 7270 Davos Platz, Switzerland. E-mail: martin.stoddart@aofoundation.org

bone repair strategies (Homma *et al.*, 2013; Kon *et al.*, 2012).

Bone morphogenetic protein-2 (BMP-2) is a potent regulator of bone repair, critical in the fracture healing process, where it exerts complementary effects upon both osteogenesis and angiogenesis (Ruschke *et al.*, 2012). The morphogen upregulates osteogenic-related gene expression in osteoblasts and mesenchymal progenitors, acting principally via Smad and p38 mitogen-activated protein kinase signalling pathways (Luu *et al.*, 2007; Nishimura *et al.*, 1998). Moreover, BMP-2 also appears to be involved with osteoprogenitor cell recruitment from the periosteum during bone healing (Wang *et al.*, 2011). With respect to angiogenesis, BMP-2 may stimulate vascular endothelial growth factor expression in osteoblasts (Deckers *et al.*, 2002) and the chemotaxis of endothelial progenitor cells (Raida *et al.*, 2006). Given its crucial role in osteogenesis, BMP-2 has been used for almost two decades to induce heterotopic ossification *in vivo* (Kusumoto *et al.*, 1998; Vogelin *et al.*, 2005; Yoshida *et al.*, 1998). Since then, many groups have explored the regenerative potential of the growth factor to repair bone in various animal models of large segmental bone defects, long bone fractures, calvarial defects and in spinal fusion (Axelrad and Einhorn, 2009). BMP-2 has been used clinically for spinal fusion (Carreon *et al.*, 2009; Hodges *et al.*, 2012; Katayama *et al.*, 2009; Slosar *et al.*, 2007) and in patients following dental implant extraction (Fiorellini *et al.*, 2005). However, adverse effects, attributed to using high quantities and uncontrolled release of the growth factor, have also been reported (Carragee *et al.*, 2011; Lubelski *et al.*, 2013; Mesfin *et al.*, 2013).

Growth factor delivery to bone may be achieved using both non-viral and viral gene delivery systems (Evans, 2012). Such approaches offer potential advantages over application of recombinant protein, including post-translational modification and the localized, sustained and controllable nature of transgene expression. Delivery of BMP-2 via adenoviral vectors has been shown to promote bone healing in both rabbit (Baltzer *et al.*, 2000) and rat (Betz *et al.*, 2006) segmental femoral defect models. Tet-on and Tet-off control systems allow for tuneable control of transgene expression, which is attractive for the delivery of growth factors in a clinical setting. Promising results have recently been reported following combined MSC transplantation with retroviral delivery of stromal cell derived factor (SDF-1) under a Tet-off control system in a tibial intramedullary transplantation lethally irradiated mouse model (Herberg *et al.*, 2015).

In the case of large bone defects, tissue engineering aims to initiate bone healing by providing a mechanically stable environment, vasculature, inorganic mineral and a source of osteoprogenitor cells or osteoblasts to generate bone matrix and initiate tissue repair. Here, we report a combinatorial tissue engineering approach to repair critically sized defects in nude rats. We hypothesized that bone defect healing could be enhanced by doxycycline inducible adenoviral delivery of BMP-2. Two viral delivery methods were investigated (i) direct application and (ii)

pre-coated MBCP granules (Table 1). In both *in vitro* and *in vivo* studies, virus control groups were included, whereby the vector was delivered in the absence of doxycycline, thus transgene expression was not induced. Human MSCs were used as an osteoprogenitor cell source. MBCP provides an osteoconductive surface, mechanical strength and stiffness in addition to promoting structural integrity within the defect. Here we used fibrin to provide a physiologically relevant cell carrier in order to retain cells, MBCP granules and the vector within the defect site and promote integration with nascent tissue.

Methods

Adenoviral vector

The Tet-on adenoviral shuttle vector was constructed by cloning the tetracycline response element (TREtight) and a polyadenylation signal into the adenoviral shuttle vector pDC312 (Microbix, Toronto, Canada). The cDNA coding for human BMP-2 was subcloned into the SmaI site of the 'Tet-on' shuttle vector. Subsequently, an expression cassette carrying the human cytomegalovirus immediate early promoter, the cDNA for the reverse transactivator (rtTA2S-M2) (Gossen *et al.*, 1995) and a polyadenylation signal was directionally cloned into the BglII and the Klenow enzyme filled-HindIII site downstream of the BMP-2 Tet-on vector. Plasmid DNA vector integrity was verified by DNA sequencing. Recombinant adenoviral vectors were obtained by site-specific Cre recombination between the loxP site of the shuttle vector and the loxP site of the backbone vector pBHG10loxΔE1,E3Cre (Microbix) using the calcium phosphate precipitation method on 293 cells (Graham and van der Eb, 1973). Plaques were isolated, purified and expanded on 293 cells (Microbix). Adenoviral vectors were purified by double caesium chloride gradient centrifugation and subsequent desalting with PD-10 Column Sephadex G-25 M (GE Healthcare, Munich, Germany). Titres were determined by endpoint dilution assay to obtain a biological titre (pfu/ml) (Anton *et al.*, 2012).

MSC isolation and *in vitro* expansion

Vertebral body bone marrow aspirate was obtained from a 22-year-old male with informed consent and full ethical

Table 1. Control and experimental group allocation

Groups	Name	Vector delivery	Doxycycline
Control			
1	Control	-	-
2	Ad control	Direct	-
3	Pre-C Ad control	Pre-coated ceramic	-
4	Doxycycline control	-	625 mg/kg feed
Experimental			
5	Ad + Dox	Direct	625 mg/kg feed
6	Pre-C Ad + Dox	Pre-coated ceramic	625 mg/kg feed

approval (KEK Bern 126/03). Mononuclear cells were isolated using a standard density centrifugation method. Briefly, bone marrow aspirate was diluted 1:3 in phosphate-buffered saline (PBS; Sigma, St Louis, MO, USA), filtered through a 70 μm cell strainer, layered on to Histopaque-1077[™] (Sigma, 10771) and centrifuged at 800 g for 20 min at room temperature without braking. The interphase, containing the mononuclear cell fraction, was collected and washed twice in culture medium: alpha-MEM (Gibco, Zug, Switzerland), 10% fetal calf serum (Gibco) and 0.05% penicillin and streptomycin (Gibco) and a cell count performed using a Scepter[™] 2.0 Automated Cell Counter (Millipore, Darmstadt, Germany). Mononuclear cells were cultured at a density of 50 000 cells/cm² in culture media supplemented with 5 ng/ml basic fibroblast growth factor (Fitzgerald, North Acton, MA, USA) at 37°C and 5% CO₂. MSCs were cultured in the presence of fibroblast growth factor, as this is known to be a potent mitogen and maintains multipotency (Bianchi *et al.*, 2003; Martin *et al.*, 1997; Solchaga *et al.*, 2005). A media change was performed after 4 days to remove non-adherent cells with subsequent media changes three times a week. MSCs were stored in liquid nitrogen and used at passage 2 for subsequent *in vitro* and *in vivo* experiments.

***In vitro* study**

MBCP granules comprising 60% hydroxyapatite and 40% calcium phosphate, pore size between 300 and 600 μm , were used in the study (BiomatIntle, Vigneux de Bretagne, France). MSCs were transduced in three dimensions as previously described (Neumann *et al.*, 2013) with Ad-tetBMP-2 in combination with MBCP and fibrin to determine transgene expression *in vitro*. In both *in vitro* and *in vivo* studies, virus control groups were included, whereby the vector was delivered in the absence of doxycycline, thus transgene expression was not induced. Groups were as follows: Group 1 Control: cells + fibrin + granules; Group 2 Ad control: cells + fibrin + granules + virus; Group 3 Pre-C Ad control: cells + fibrin + granules pre-coated with virus; Group 4 Doxycycline control: cells + fibrin + granules + doxycycline; Group 5 Ad + Dox: cells + fibrin + granules + virus + doxycycline; Group 6 Pre-C Ad + Dox: cells + fibrin + granules pre-coated with virus + doxycycline. Each construct contained 0.5×10^6 MSCs \pm 100 mg MBCP granules. Tet-on AdBMP-2 was used at 10 pfu/cell in serum-free high glucose DMEM media (Gibco). 100 mg granules were pre-wet with 50 μl DMEM media \pm virus. Fibrinogen and thrombin (Baxter, Vienna, Austria) were used at final concentrations of 16 mg/ml and 2 U/ml, respectively. For each construct, 0.5×10^6 MSCs were resuspended in 75 μl fibrinogen and mixed with the granules. Finally, a 75 μl volume of thrombin was applied to each construct to initiate polymerization. Constructs were incubated at 37°C for 30 min to ensure homogeneous polymerization prior to incubation with

culture media [DMEM high glucose 4.5 g/l, 1% Insulin transferrin selenium (ITS) (Corning, New York, NY, USA), 50 $\mu\text{g/ml}$ ascorbate-2-phosphate (Sigma) and 100 μM ϵ -aminocaproic acid (Sigma)]. Cell supernatant was collected at day 2 as a baseline control for BMP-2. Subsequent media changes, performed every 3 days, were supplemented with 0.5 or 1 g/ml doxycycline (Sigma). Cell culture supernatant was collected and media changes performed on days 2, 4, 7, 10, 13 and 16 of the experiment. Supernatant from each group was collected and stored at -20°C prior to BMP-2 enzyme-linked immunosorbent assay (ELISA). Cell survival at day 7 was determined by CellTiter-Blue[®] according to the manufacturer's instructions (Promega, Madison, WI, USA).

Bmp-2 Elisa

Secreted BMP-2 was quantified from the cell supernatant of cells transduced in three dimensions using a BMP-2 ELISA (DY355, R&D Systems, Minneapolis, MN, USA) according to the manufacturer's instructions. All steps were performed at room temperature. Briefly, the BMP-2 monoclonal antibody was diluted to 1 $\mu\text{g/ml}$ in PBS and incubated with the plate overnight. After washing three times with 0.05% PBS-Tween, plates were blocked with 1% bovine serum albumin in PBS for 2 h. Supernatant was diluted in 1% bovine serum albumin in PBS, added to the wells together with BMP-2 standards and incubated for 2 h. After repeated washing in PBS-Tween, a detection antibody cocktail was applied for 2 h followed by streptavidin HRP provided in the kit for 20 min. Samples were incubated with substrate solution for 20 min in the dark prior to the addition of the stop solution. Optical density was measured using a microplate reader (Victor3 Micro Plate Reader, Perkin Elmer, Germany) at 450 nm. Readings at 540 and 570 nm were subtracted from readings at 450 nm to correct for optical imperfections in the plate.

***In vivo* study design**

The *in vivo* study was performed using 34 female, 22–24-week-old (mean body weight 233 ± 21 g) specific pathogen-free Charles River Rowett Nude rats within an AAALAC International accredited facility. Animals were group housed in Individual ventilated cages (IVC) cages in a biosafety level 2 facility before and for the duration of the study. SPF status of the animals was confirmed before surgical intervention and at euthanasia (Rat PCR Rodent Infectious Agent panels; Charles River, Sulzfeld, Germany). Animals were randomly assigned to experimental and control groups, which are defined in Table 1. Animals were checked for general health by qualified veterinarians throughout the study. All animals received standard feed prior to surgery *ad libitum* (Provimi-Kliba, extrudat 3436). After surgery, animals in groups 1–3 received standard feed and animals in groups

4–6 received feed containing doxycycline (Provimi-Kliba, feed-number: 3432.PM.PM.V20 + 1% saccharose and chocolate aroma + doxycycline at 625 mg/kg feed). Those involved in the surgery, postoperative care, radiological, computed tomography and histological analysis were blind with regards to individual group allocation for the duration of the study.

Surgery and implantation of constructs

A critically sized bone defect model in rats was used as previously described (Poser *et al.*, 2014). All groups received MCBP granules, MSCs and fibrin. AdTetBMP-2 was administered either by pre-coating the granules the day before surgery or by direct application on the day of surgery. MCBP granules were pre-wet the day before surgery with PBS with/without virus (10 pfu/cell). PBS \pm virus were applied to granules for 30 min, then removed and discarded. On the day of surgery, passage 2 MSCs were trypsinized and resuspended in fibrinogen. For groups 3 and 4, AdTetBMP-2 was mixed into the thrombin approximately 2 h before implantation. Immediately before implantation, MSCs in fibrinogen were combined with the granules and thrombin and implanted into the defect site (Figure 1). In order to suitably fit the 4 mm defect, construct size was modified from the *in vitro* experiment and thus comprised: 30 mg MCBP granules, 1.5×10^5 MSCs, 30 μ l fibrinogen and 30 μ l thrombin \pm virus.

Surgery was performed under a laminar flow hood. Anaesthesia was induced with isoflurane Baxter®/Baxter AG/55999 at 3% and maintained thereafter at 1.5–1.8% in oxygen at 0.6–1 l/min. Animals received 0.1 mg/kg buprenorphine (Temgesic®, Reckitt Benckiser, Wallisellen, Switzerland) subcutaneously prior to surgery. Animals were placed in ventral recumbency and the left femur aseptically prepared. A curved skin incision was made from the base of the tail to the stifle. The subcutaneous fascia lata was sharply incised and the *M. quadriceps* and *M. biceps femoris* separated bluntly to expose the lateral aspect of the femur, avoiding manipulation of the sciatic nerve. A PEEK plate (RIS.602.100, RatFix plate 8 hole, Risystem AG, Davos, Switzerland) was fixed to the dorsolateral surface of the femur using six self-cutting locking titanium screws (RIS.402.120, RatFix shoulder screw 0.70 \times 5.70 mm) with the centre of the plate at the distal level of the lateral

femoral crest. 4 mm defects were created in the centre of the plate by two osteotomies using a Gigly hand saw (RIS.590.110, Gigly wire saw 0.44 mm) and jig (RIS.302.104, RatFix drill and saw guide 4 mm at 23 mm). Defects were filled according to group allocation, with the surgeon blinded. Fascia and skin were closed in a continuous pattern with # 5-0 Vicryl rapide (Ethicon, Diagem, Belgium). Animals received 3 ml warmed Ringer's solution and 0.1 mg/kg buprenorphine (Temgesic®) subcutaneously after surgery. Postoperative analgesia was administered for 7 days in the animals' drinking water (Dafalgan® Sirup 3%, Bristol-Myers Squibb SA, Cham, Switzerland) at 7 ml/100 ml water. Weight was recorded at surgery and weekly thereafter. Animals were euthanized after 12 weeks by carbon dioxide.

Radiographs

Lateral radiographs were taken postoperatively, at 6 weeks and at 12 weeks post-mortem (Trauma Diagnost, Philips Medical Systems, Hamburg, Germany). Radiographs were scored independently by two blinded assessors using a grading system that considered both the granularity and the abundance of radiodense material with the defect site and the degree of bridging (Figure S1). The combined radiograph score presented is the mean of both assessors' scores.

Micro-computed tomography

Animals were scanned post-mortem at 12 weeks (VivaCT40, Scanco Medical, Bruttisellen Switzerland). In addition, three animals from group 1 were scanned under anaesthesia immediately postoperatively and after 6 weeks. One thousand projections per scan were acquired at 70 kV, 114 μ A and 200 ms integration time. Slices were reconstructed across an image matrix size of 2048 \times 2048 voxels, with a nominal voxel size of 19 μ m. A region of interest (ROI) for image analysis was defined using a postoperative scan (reference scan). The reference scan was first re-oriented to align the femur in the z-axis. A cylindrical ROI, diameter 7.5 mm and centred on the bone axis, was defined by interpolations between two circular contours at both osteotomy sites. The first and last 10 slices were deleted from the ROI to exclude surrounding bone from the analysis. The same ROI was

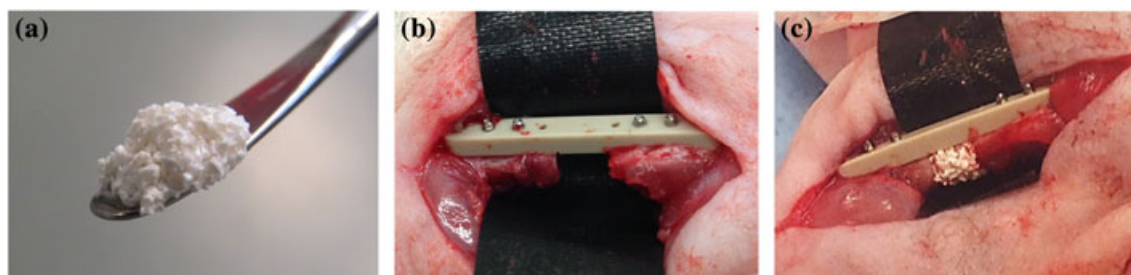


Figure 1. Photographs of (A) mesenchymal stromal cell fibrin-MCBP® construct directly after polymerization and of the animal surgery (B) after plate fixation and (C) following implantation of the construct.

applied to all scans by aligning them to the reference scan. Scans were Gaussian-filtered ($\sigma = 1$, support = 2) and calcified material (including MBCP granules and calcified tissue) segmented (threshold = 370 mgHA/cm³). The volume of calcified material within the defect was computed from the number of segmented voxels within the ROI.

Histology

After euthanasia, femurs with attached plates and the surrounding soft tissue were excised and fixed in 70% ethanol for 4 weeks. Samples were dehydrated in a series of graded alcohols to xylene prior to embedding in methyl methacrylate (Sigma). Serial cross-sections of approximately 250 μm were taken using a saw microtome (Leica SP 1600 saw microtome, Leica AG Wetzlar, Germany). Sections were glued on to opaque Plexiglas slides, ground and polished to a thickness of approximately 100 μm (Exakt Micro Grinding System, Exakt Apparatebau, Norderstedt, Germany). Sections were treated with 1% formic acid and stained with 15% Giemsa solution (Fluka Buchs, Switzerland), rinsed and further stained with a 1% eosin solution (Sigma) for histological analysis. Images were taken using a Zeiss Axioplan 2 fluorescence microscope. The images presented show the best defect healing observed for each group. The amount of newly formed bone within the defect site was quantified using Adobe Photoshop CS5 image analysis software. Briefly, a ROI of 3 \times 4.5 mm was created between the two most internally fixed screws, which defined the defect area. Thresholding parameters were used to create a mask of newly formed bone, which excluded the granules and other soft tissues (Figure S2). By calibrating to the scale of the image, the percentage area of the defect occupied by bone could be automatically quantified.

Bending stiffness

In order to determine bending stiffness, the micro-computed tomography scan was cropped to include only the volume between the inner screws of the fixation plate. This was then converted into a micro-finite element model with a conversion from grey scale to elastic modulus as described by Homminga *et al.* (2001). A wedge displacement of 1.5° in the plane of the screws was applied to both ends of this model. This loading created a bending moment and potentially also an axial loading (compression or tension) if the bone was not perfectly aligned and balanced in the centre of the image. To calculate the bending moment, the average axial load was subtracted from each end, the remainder was then multiplied by the distance from the centre of bending and integrated across the surface. Due to the small angle, the radius of the bend was very large, the alignment of the bone within the image had only a small effect (0.05%) on the bending radius, a theoretical radius passing through the model centre was used for each

image. This allowed us to calculate the bending stiffness EI (Young's modulus \times moment of inertia).

Statistics

Both *in vitro* and *in vivo* data were non-normally distributed, as determined by the D'Agostino-Pearson test for normality and variances not equal for all outputs as determined by Levene's test. CellTiter-blue® and BMP-2 ELISA data are presented as means \pm standard error of the mean. Data from individual animals are presented as scatterplots for each group for radiograph score, micro-computed tomography and histological bone formation, with error bars representing the interquartile range of the group. A statistical analysis was performed using GraphPad Prism 6. A single outlier in group 5 (Ad + Dox) was identified following micro-finite element analysis and thus excluded from the analysis of bending stiffness. Differences between groups were tested for statistical significance using Mann-Whitney tests between two groups and Kruskal-Wallis one-way analysis of variance test between more than three groups.

Results

Doxycycline inducible BMP-2 expression by MSCs *in vitro*

MSC viability in the presence or absence of adenovirus with/without doxycycline was firstly investigated *in vitro*. CellTiter-blue® revealed that MSCs proliferated within the constructs in all groups (Figure 2A). The mean fluorescence intensity of CellTiter-blue® was significantly higher at day 7 compared with day 0 in controls ($p = 0.0043$) and in all virus groups (Ad: 0.032, Ad + Dox: $p = 0.032$, Pre-C + Dox: $p < 0.0001$; Kruskal Wallis) with the exception of group 3 (Pre-C + Ad).

The amount of secreted BMP-2 was compared between all groups by ELISA. BMP-2 was detected in the culture media of Ad + Dox transduced MSCs at day 4 at 238 ± 41.7 pg/ml 2 days after doxycycline supplementation had commenced (Figure 2B). Conversely transgene expression was not detectable in the Pre-C + Dox group until day 7 (254 ± 178 pg/ml Figure 2B). In both Ad + Dox and Pre-C + Dox groups BMP-2 increased during 16 days of culture with levels remaining consistency lower when the virus had been pre-coated on to the granules compared with direct application. BMP-2 was detected at significantly higher levels at day 7 in the Ad + Dox group (1212 ± 172 pg/ml) compared with the Pre-C + Dox group (254 ± 178 pg/ml Kruskal-Wallis $p = 0.0007$). BMP-2 detected in virus groups treated with 0.5 ng/ml doxycycline was consistently lower compared with groups treated with 1 ng/ml doxycycline and was statistically significant at day 4 ($p = 0.0007$ Kruskal-Wallis Figure 2 B). Importantly no secreted BMP-2 was detected in either doxycycline-free or un-transduced controls. Together

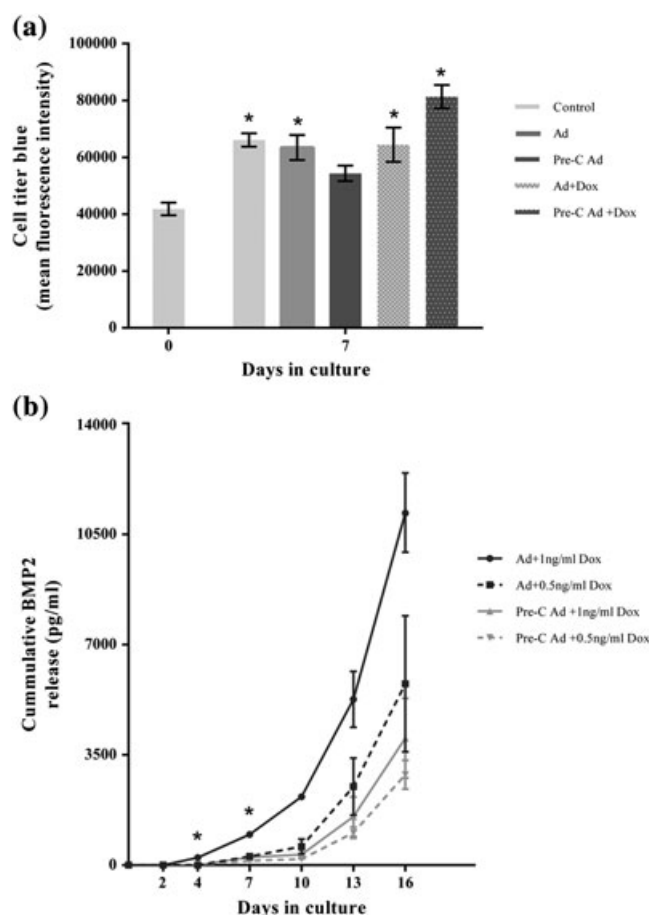


Figure 2. (A) Viability of transduced/untransduced mesenchymal stromal cells (MSCs) encapsulated within fibrin gels as determined by CellTiter-Blue® at day 7. (B) Quantitation of BMP-2 from the secretome of MSCs transduced directly or by pre-coating MBCP® with adenovirus over 16 days. Media was supplemented with doxycycline (0.5 vs. 1 ng/ml) from day 2 onwards. Data presented are means \pm standard error of the mean, * $p < 0.05$, ** $p < 0.005$

these data demonstrate that *in vitro* transgene expression is (i) delayed and more gradual by pre-coating the granules with virus and (ii) tuneable via modulation of doxycycline concentration

In vivo study results

Surgeries were performed successfully without major complication. Two animals were euthanized early due to screw failure and were therefore excluded from the study. The majority of animals gained weight postoperatively, were healthy and exhibited normal behaviour, as observed by qualified veterinarians. There was some variation in weight gain and final weights between animals, but no significant differences between groups (mean weight at euthanasia group 1: 248 ± 14 g, group 2: 243 ± 25 g, group 3: 250 ± 13 g, group 4: 255 ± 15 g, group 5: 243 ± 14 g, group 6: 243 ± 28 g).

Radiology

Radiographs taken directly postoperatively and after 12 weeks showed improved defect healing in AdTetBMP-2 groups compared with all control groups (Figure 3A–L). Inter-assessor agreement on the

radiographic scoring system was fair (Kappa statistic 0.262). Significantly higher radiograph scores were observed in Ad + Dox and Pre-C Ad + Dox groups compared with virus control groups without doxycycline administration (4.29 ± 1.27 vs. 2.86 ± 0.78 , Mann Whitney, $p = 0.0033$, Figure 3M).

When assessing the two viral delivery groups separately, radiological assessment scores of the defect site at 12 weeks were higher when the vector was applied directly (Ad + Dox: 4.50 ± 1.30) compared with the respective virus control group without doxycycline (Ad control: 2.92 ± 1.15). Similarly, significantly higher radiograph scores were seen when MBCP granules were pre-coated with the virus (Pre-C Ad + Dox: 4.08 ± 1.32) compared with the respective virus control group without doxycycline (Pre-C Ad: 2.80 ± 0.27 , Kruskal-Wallis, $p = 0.0325$, Figure 3N). No difference in radiological score was apparent when comparing direct vs. pre-coated ceramic granules as methods of vector delivery.

Micro-computed tomography

Postoperative computed tomography showed that MBCP granules remained in place within the defect site following surgery and for the study duration (Figure 4A, B). The total mineralized tissue volume was measured

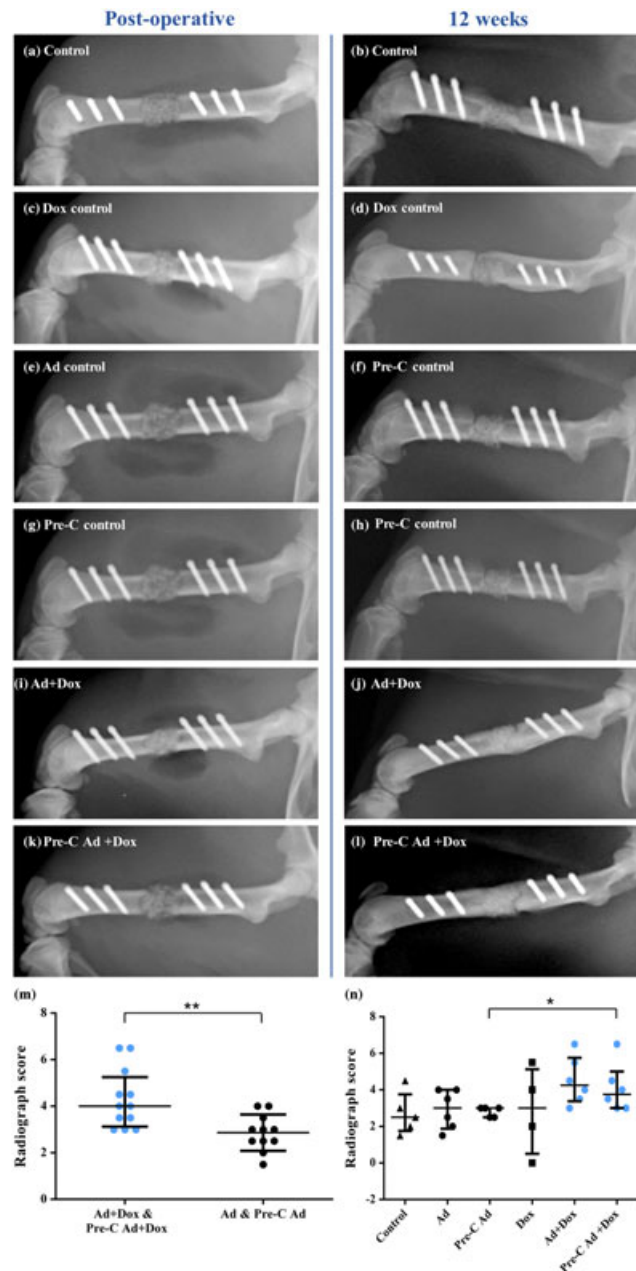


Figure 3. Radiographs taken (A,C,E,G,I,K) postoperatively and (B,D,F,H,J,L) 12 weeks after surgery. (M, N) Radiograph scoring at 12 weeks determined by two blinded, independent assessors (see Figure S1 for scoring details). Box plots present scores from each animal with the interquartile range, * $p < 0.05$, ** $p < 0.005$. (M) Combined data from both virus groups (Ad and Pre-C + Dox) compared against the two corresponding (-)doxycycline controls. (N) Data presented for each of the six groups. Groups: Control ($n = 5$); Ad: AdTetBMP-2 control ($n = 6$); Pre-C Ad: MBCP® pre-coated with AdTetBMP-2 ($n = 5$); Dox: doxycycline control ($n = 4$); Ad + Dox: AdTetBMP-2 + doxycycline ($n = 6$); Pre-C Ad + Dox: MBCP pre-coated with AdTetBMP-2 + doxycycline ($n = 6$).

above 370 mgHA/cm³. Considering all groups, animals exhibiting the best defect repair were in the Ad + Dox and Pre-C Ad + Dox groups (Figure 4E, F). Three-dimensional reconstructions showed extensive integration of granules and newly formed bone with native bone in these animals (Figure 4B–F). There was a trend towards increased mineralized tissue volume within the defect site in virus groups compared with (-) doxycycline controls, although this was not statistically significant (Figure 4G). As it was not possible to reliably discriminate (in terms of segmentation) between implanted ceramic and callus, differences between groups in terms of remodelled ceramic would not be reflected in the computed tomography data. No significant difference

in mineralized tissue volume was seen between the two viral delivery methods (Figure 4H).

Histology

No adverse tissue reaction or ectopic ossification in the surrounding tissue of the defect site was seen histologically in any of the animals post-mortem (Figure 5A–F). Defect sites in control groups contained mostly fibrous tissue and a small amount of new bone (Figure 5A–D), whereas defects were mostly filled with new bone and a comparatively small amount of fibrous tissue in treatment groups (Figure 5E, F). MBCP granules integrated with both nascent and newly formed

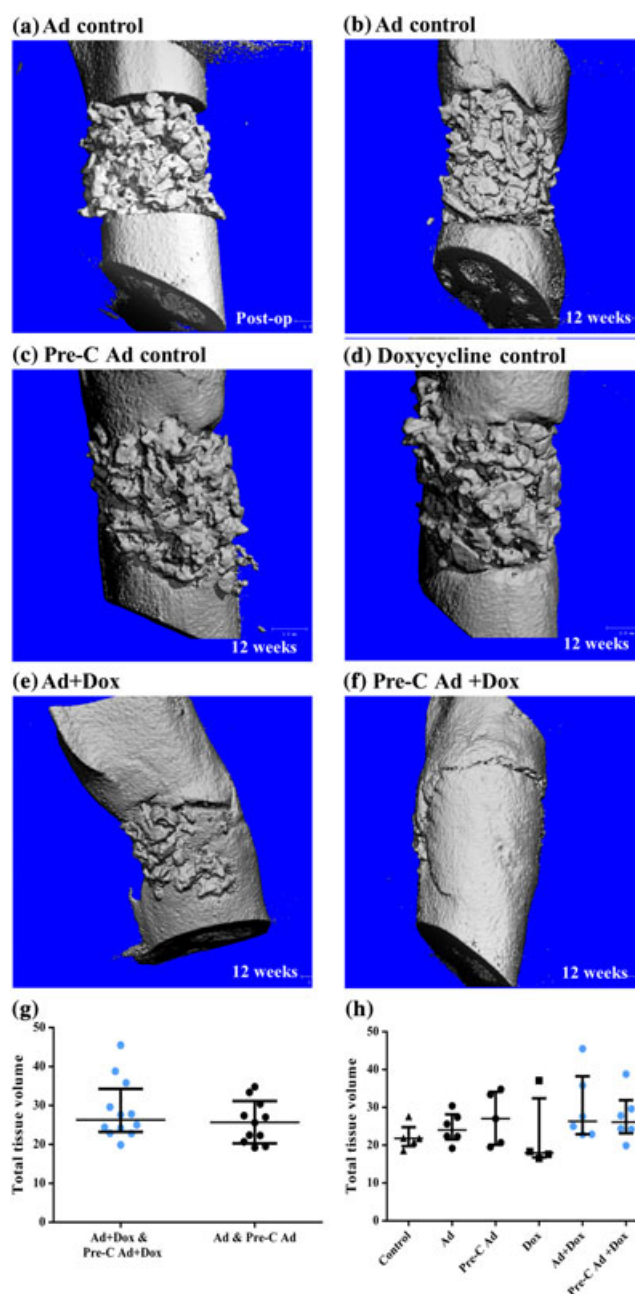


Figure 4. Micro-computed tomography three-dimensional reconstructions and quantitation of total tissue volume $> 370 \text{ mgHA/cm}^3$ within the defect site. Ad controls (A) postoperative and (B) 12 weeks after surgery. (C) Pre-C Ad control, (D) doxycycline control, (E) Ad + Dox, (F) Pre-C Ad + Dox 12 weeks after surgery. (G, H) Box and whisker plots of total tissue volume in all groups at 12 weeks postoperative. Box plots present scores from each animal with the interquartile range. (G) Combined data from both virus groups (Ad and Pre-C + Dox) compared against the two corresponding (-)doxycycline control groups. (H) Data presented for each of the six groups. Groups: control ($n = 5$); Ad: AdTetBMP-2 control ($n = 6$); Pre-C Ad: MBCP® pre-coated with AdTetBMP-2 ($n = 5$); Dox: doxycycline control ($n = 4$); Ad + Dox: AdTetBMP-2 + doxycycline ($n = 6$); Pre-C Ad + Dox: MBCP pre-coated with AdTetBMP-2 + doxycycline ($n = 6$).

vascularized bone within the defect site in all groups, which was more evident in animals where defect filling was highest (Figure 5E, F). The histology presented in Figure 6 shows the most superior healing of the defect site from an AdTetBMP-2 treated rat (Ad + Dox, group 5). Newly formed bone was vascularized with osteoblasts on the endosteal surface and osteocytes occupying lacunae were clearly visible (Figure 6A). The presence of cartilaginous tissue and hypertrophic chondrocytes in animals demonstrating the highest levels of defect healing suggested that bone formation had occurred via endochondral ossification (Figure 6B). Bone marrow compartments were observed within the defect sites of

four of 20 control animals and eight of 12 treatment (Ad/Pre-C Ad + Dox) animals (Figure 6C). The total area of newly formed bone within the defect site was semi-quantified using thresholding and masking tools with Adobe Photoshop CS5 (Figure S2). Semi-quantitative analysis of *de novo* bone formation revealed that the percentage of bone within the defect site was significantly greater in Ad + Dox and Pre-C Ad + Dox groups compared with virus controls without doxycycline administration ($29.09 \pm 8.32\%$ vs. $22.04 \pm 4.69\%$, $p = 0.0267$, Mann-Whitney, Figure 5G). There was no significant difference between individual groups and when comparing the two vector delivery approaches (Figure 5H).

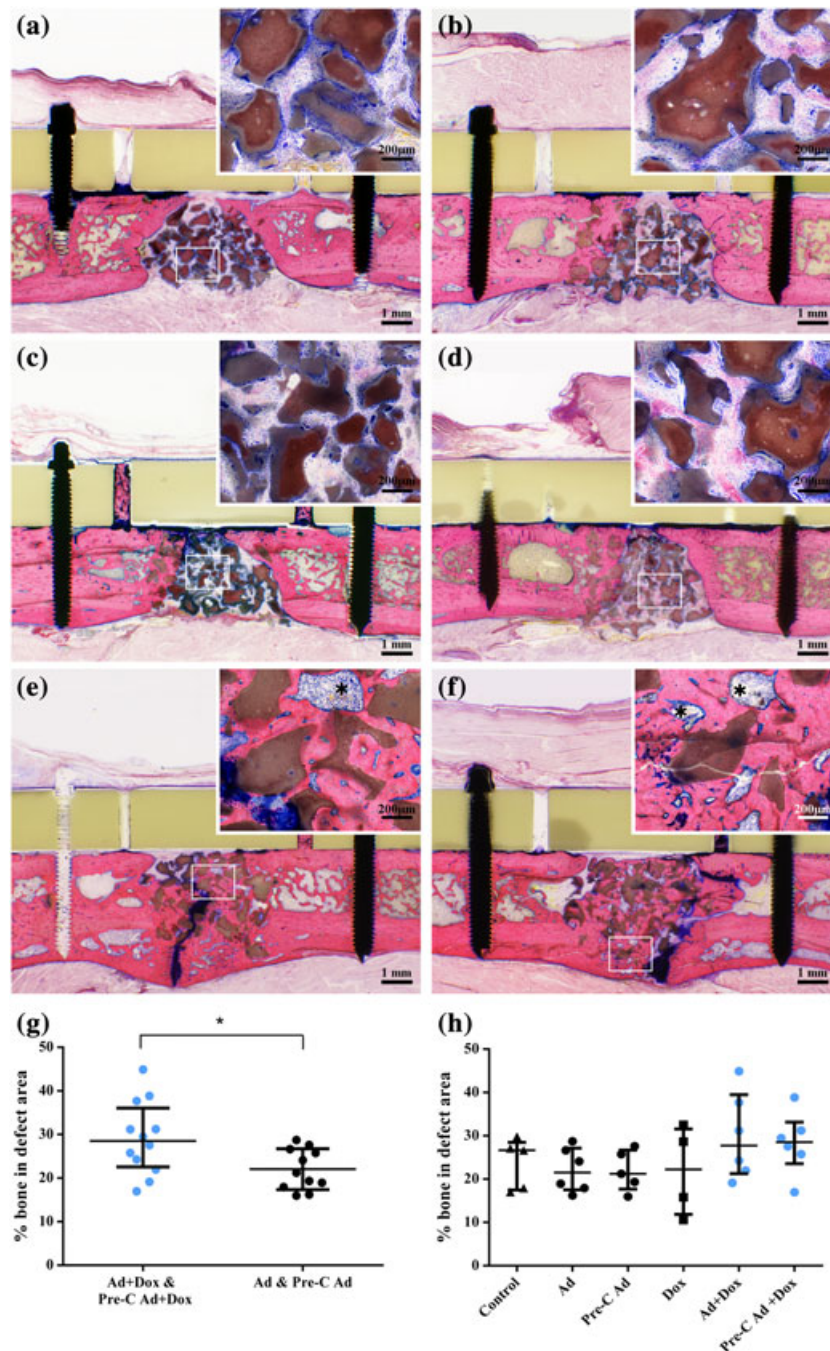


Figure 5. Histological analysis of the defect area and quantitation of *de novo* bone formation. Giesma eosin stained sections from (A) control and (B) Ad control, (C) Pre-C control, (D) doxycycline control, (E) Ad + Dox, (F) Pre-C Ad + Dox. Asterisks indicate bone marrow compartments within the defect site. (G, H) Box and whisker plots of *de novo* bone formation for each animal as a percentage of the total defect site area at 12 weeks, semi-quantified from Giemsa eosin-stained sections. (G) Combined data from both virus groups (Ad + Dox and Pre-C Ad + Dox) compared with the two corresponding virus (-doxycycline) controls. (H) Data presented for each of the six groups. Groups: control ($n = 5$); Ad: AdTetBMP-2 control ($n = 6$); Pre-C Ad: MBCP® pre-coated with AdTetBMP-2 ($n = 5$); Dox: doxycycline control ($n = 4$); Ad + Dox: AdTetBMP-2 + doxycycline ($n = 6$); Pre-C Ad + Dox: MBCP pre-coated with AdTetBMP-2 + doxycycline ($n = 6$).

Bending stiffness

Bending stiffness EI, determined by micro-finite element analysis of micro-computed tomography images, was greater, although not significantly so, following delivery of AdTetBMP-2 + doxycycline compared with (-) doxycycline controls (224 ± 136.9 vs. 148.5 ± 48.2 Nmm², Figure 7A). No significant difference in bending stiffness was apparent between the direct vs. virus pre-coating vector delivery approach (Figure 7B).

Discussion

In this study, we investigated whether the healing of large femoral bone defects could be improved by inducible adenoviral delivery of BMP-2 using a biomaterial-mediated gene delivery approach. This was carried out by combining human MSCs, fibrin, a porous ceramic (MBCP) together with a doxycycline inducible Tet-on adenoviral vector encoding the BMP-2 transgene. Two viral delivery methods were tested (i) direct application and (ii) pre-coated MBCP granules.

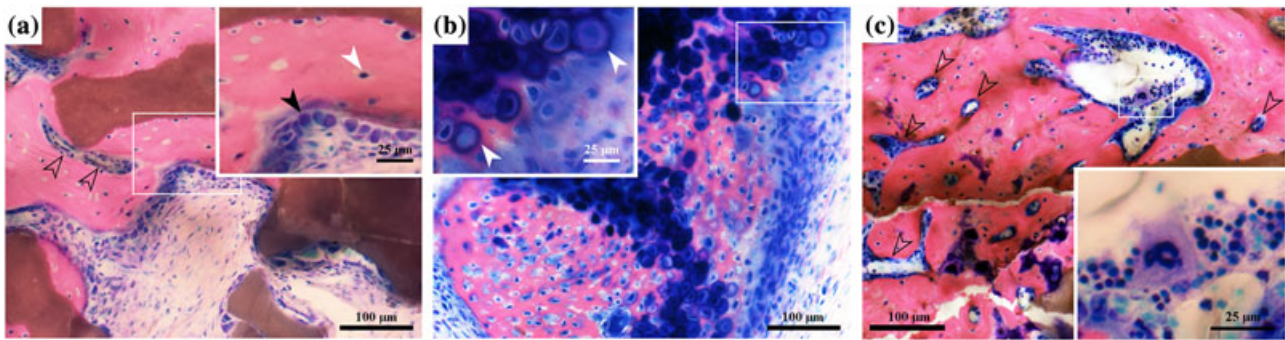


Figure 6. Histology of the most superior healing of the defect site from an AdTetBMP-2 treated rat (Ad + Dox, group 5). (A) Direct integration of the MBCP® granules with new bone. Blood vessels (open black arrow heads), osteoblasts (see inset: black arrow head) and osteocytes in lacunae can be identified (see inset: white arrow head). (B) The presence of cartilaginous tissue and hypertrophic chondrocytes (see inset: white arrow heads) suggests bone formation via an endochondral route. (C) Extensive vascularization (open black arrow heads) and bone marrow compartments were observed in the defect sites of AdTetBMP-2 + doxycycline treated animals.

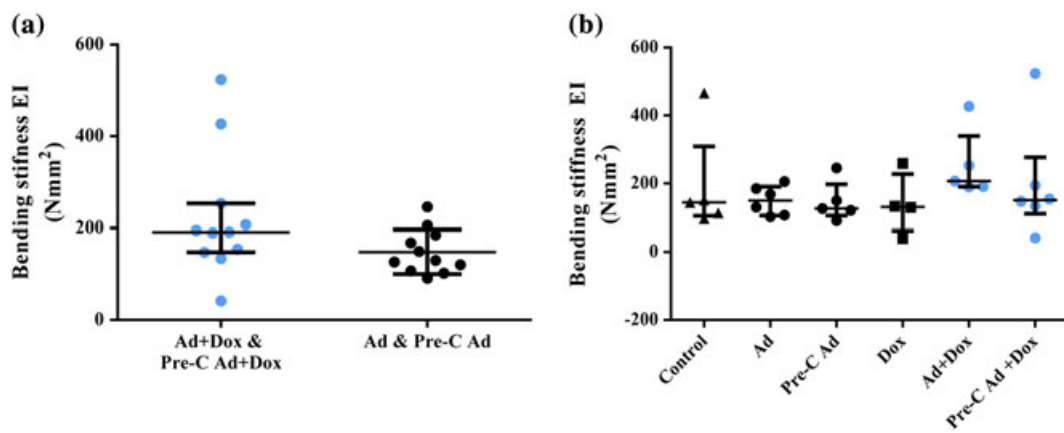


Figure 7. Bending stiffness as determined by micro-finite element modelling. (A) Combined data from both virus groups (Ad + Dox and Pre-C Ad + Dox) compared with the two corresponding virus (-)doxycycline controls. (B) Data presented for each of the six groups. Groups: control (n = 5), Ad: AdTetBMP-2 control (n = 6); Pre-C Ad: MBCP® pre-coated with AdTetBMP-2 (n = 5); Dox: doxycycline control (n = 4); Ad + Dox: AdTetBMP-2 + doxycycline (n = 6); Pre-C Ad + Dox: MBCP pre-coated with AdTetBMP-2 + doxycycline (n = 6).

In vitro work confirmed the effectiveness of adenoviral transduction of MSCs in three dimensions, as previously reported by our group (Neumann *et al.*, 2013). Furthermore, there was no evidence of leaky BMP-2 expression in the absence of doxycycline. In our *in vivo* study, the combined results of micro-computed tomography, radiology and histology demonstrated no to minimal healing in control groups 1–3 (no virus, AdTetBMP-2 without doxycycline, pre-coated granules + AdtetBMP-2 without doxycycline) and improved healing in experimental groups 5 and 6 (AdTetBMP-2 + doxycycline, pre-coated granules + AdtetBMP-2 + doxycycline). These results affirm the suitability of our large bone defect model and the reliability of the Tet-on control system. Improved bone healing was observed in the majority of animals that had received either direct application of the virus or where MBCP granules had been pre-coated and doxycycline had been applied to induce transgene expression. Although radiological and histological data showed significantly greater bone healing in virus groups, this was not the case for micro-computed tomography. Due to similarity in density, it was not possible to discriminate between ceramic and callus in terms of segmenting micro-

computed tomography data, thus ceramic and remodelled ceramic replaced by callus, were not distinguishable. Considering this and our other data, we postulate that the micro-computed tomography data probably underestimated the degree of remodelling and healing in virus groups. Notably, we observed a trend of higher bending stiffness, as determined by micro-finite element analysis in virus groups – demonstrating that transgene expression was effective in augmenting the biomechanical properties of the repair tissue. Two animals in each of the two virus groups demonstrated superior defect filling, bridging and integration of vascularized woven bone. Hence, we observed a range in biological response to vector administration. It may be that this variation in outcome was attributable to the nature of doxycycline administration, discrete anatomical variation and differences in individual recovery rate of the animals postoperatively. Doxycycline was administered in the animals' feed and as the animals were grouped housed it was not possible to know exactly how much doxycycline each animal had received. Doxycycline may also be administered via drinking water, but this has been shown to be less reliable compared with feed and often results in dehydration (Cawthorne *et al.*, 2007). Furthermore, we

wanted to limit handling of the immune-compromised animals as much as possible to reduce infection risk. The availability of doxycycline at the defect site is also dependent upon the nascent vasculature, thus variation in vascularity in and around the defect site may have also contributed to differences in healing rate between these animals. Overall, our data show that our vector was effective in mediating transgene expression and that this resulted in a subsequent improvement in bone defect healing. Further investigation of the tuneable nature of this vector by modulation of doxycycline dose, administered intravenously, will be required to confirm the suitability of this vector system in a clinical setting.

Previous works have reported the successful use of lentiviral (Hsu *et al.*, 2007) and retroviral vectors (Herberg *et al.*, 2015) for gene delivery to segmental bone defects. Here, we report the first *in vivo* study of its kind utilizing a non-integrating Tet-on inducible adenoviral gene delivery system to bone. Our results suggest that this viral gene transfer method may have the potential to augment the repair of large, non-healing bone defects in man. Our bone defect model and novel gene delivery system may provide a powerful standardized tool for optimizing the delivery and release of BMPs and other growth factors in large bone defects. Specifically, the tuneable nature of this system may allow fine control over transgene expression, which would be very useful in a clinical setting where patient response and recovery to intervention is variable. This may offer a novel therapy for the treatment of large segmental bone defects resulting from trauma or tumour resection.

In a previous study, the murine C3H10T1/2 cell line, genetically altered to express BMP-2 under the control of a tetracycline-regulated vector induced bone formation in tibial segmental defects in osteopenic mice (Moutsatsos *et al.*, 2001). In the aforementioned study, significant overproduction of bone was observed using genetically engineered cells. None of the animals in the current study demonstrated over-production of bone. Additionally, adenoviral gene delivery offers the benefit that the virus is non-incorporating, thus subsequent progeny will not over-express the transgene, facilitating more controllable growth factor expression and lessening safety concerns.

This study demonstrates proof-of-concept for an 'off-the-shelf' biomaterial-mediated approach of viral gene delivery to bone. Our vector was retained on MBCP granules for approximately 24 h following coating and upon *in vivo* delivery demonstrated comparable bioactivity compared with application of the vector at the time of implantation. Importantly, we did not see any difference between direct application vs. granules pre-coated with virus in terms of healing response. This suggests that both direct and in-direct vector application may be equally as effective in inducing repair. Other groups have successfully demonstrated long-term bioactivity of adenoviral vectors when incorporated with hydroxyapatite (Hu *et al.*, 2007) and for adeno-associated virus when freeze-dried on to cortical bone allograft (Ito *et al.*, 2005) and on to hydroxyapatite, tri-calcium

phosphate and titanium alloy (Nasu *et al.*, 2009). In future work, we plan to assess longer term bioactivity of our vector after lyophilizing to MBCP.

Osteoinductive ceramics, including hydroxyapatites (Ripamonti, 1991; Yamasaki and Sakai, 1992) and biphasic calcium phosphates (Yang *et al.*, 1996; Yuan *et al.*, 2002), may induce ectopic ossification intramuscularly and are associated with intramembranous ossification when implanted into long bone defects (Barradas *et al.*, 2011). Conversely, endochondral ossification is typically observed with the application of BMP-2 (Paralkar *et al.*, 1991; Reddi and Cunningham, 1993). The use of BMP-2 favours an endochondral ossification route that is considered favourable for the functional repair of long bone defects (Bahney *et al.*, 2014; Jukes *et al.*, 2008; Scotti *et al.*, 2010). In this study, the presence of cartilaginous tissue in the defect sites of virus-treated groups suggests that bone formation had occurred by endochondral ossification, supporting the effectiveness of our viral vector to induce transgene expression *in vivo*. Based upon the effectiveness of viral transduction seen in our *in vitro* studies, we postulate that AdTetDox transduced implanted human MSCs. However, it is also possible that the virus transduced resident cell populations in the defect site, such as osteoprogenitors, osteoblasts (Baltzer *et al.*, 1999) and endothelial cells (Wang *et al.*, 1999). Importantly, we did not observe any ectopic ossification in tissue surrounding the defect, suggesting that virally transduced cells were localized to the defect site and that an appropriate level of BMP-2 expression had been achieved. We postulate that the use of a fibrin hydrogel carrier, which has previously been shown to bind and retain adeno-associated virus *in vivo* (Breen *et al.*, 2009), aided retention of the vector. One limitation of this study is that it is not clear whether transduced MSCs promoted bone healing via a direct or indirect mechanism. Indeed, it was recently shown in a murine critically sized defect model that *ex vivo* BMP-2 expressing donor MSCs transduced with a lentivirus vector acted as protein delivery vehicles, functioning to recruit native osteoprogenitors (Pensak *et al.*, 2015). BMP-2-induced osteogenic differentiation has been extensively characterized in bone marrow-derived MSCs (Luu *et al.*, 2007; Nishimura *et al.*, 1998). Other skeletal progenitor cells, such as adipose-derived MSCs, may also provide a candidate cell source for bone repair, although osteogenic induction appears more sensitive to the timing and dose of BMP-2, as well as being dependent upon cell-biomaterial interactions and would therefore require optimization (Mehrkens *et al.*, 2012; Overman *et al.*, 2013; Tirkkonen *et al.*, 2013).

We observed low levels of BMP-2 protein secretion *in vitro* (ng/ml). Although we were not able to determine the amount of BMP-2 produced as a result of transgene expression *in vivo*, protein levels would probably also be in this range. This study suggests that low levels of the growth factor can be effective in inducing an appropriate physiological response. This is particularly relevant when comparing to alternative growth factor delivery methods. Specifically, high levels (milligram range) of

endogenously applied BMP-2 protein in the clinic has been associated with postoperative complications and adverse effects, including bony overgrowth, osteolysis and pseudarthrosis (Carragee *et al.*, 2011; Lubelski *et al.*, 2013; Mesfin *et al.*, 2013). Gene transfer of BMP-2 confers several advantages over endogenous application of recombinant protein (Evans, 2012). Importantly, with gene transfer, the protein is subject to post-translational modification. Although injection of a protein is entirely transient, adenoviral delivery has the potential to maintain gene expression of the transgene for the lifespan of the transduced cell, potentially circumventing the need for repeated application. Incorporating vectors such as lentivirus may facilitate longer lasting gene expression. However, safety concerns, including the ability to become replication competent, insertional mutagenesis and potential germline alteration, continue to challenge the clinical translation of these vectors (Matrai *et al.*, 2010).

In this study, we used human MSCs in immunocompromised rats to determine the effectiveness of the viral vector with human primary cells *in vivo* in the rat. Inflammatory processes are critical in bone regeneration, particularly in the acute phase of fracture healing. Levels of inflammatory cytokines and growth factors increase immediately following fracture, resulting in the recruitment of inflammatory cells and osteoprogenitors to the haematoma, together with vascular ingrowth (Cho *et al.*, 2002; Kitaori *et al.*, 2009; Kolar *et al.*, 2010; Kon *et al.*, 2001; Pape *et al.*, 2010). Furthermore, the relative abundance of specific immune cell subsets, namely B-cells and T-cells, changes during the fracture healing process, suggesting a temporal, co-ordinated immunoregulatory response (Konnecke *et al.*, 2014). Considering the significance of the immune response upon bone regeneration, of course our viral gene delivery system would need to be tested further using an immune-competent preclinical model. Moreover, adenoviral vectors may elicit an immune response, which, depending upon the animal model, has been shown to reduce their effectiveness *in vivo*. For example, although

it appears that the innate immune response to adenovirus is limited in rodents, a significant immune response has been observed in ovine (Egermann *et al.*, 2006) and lapine models of bone defect repair (Southwood *et al.*, 2004). For this reason, it has been proposed that an *ex vivo* transduction approach may be more suitable in large animal models (Evans, 2012). Ultimately, an autologous or allogeneic approach in immunocompetent animals would need to be performed to further investigate the overall effectiveness of this viral vector.

Here, we describe the novel use of a Tet-on adenoviral gene delivery system to bone. Doxycycline-induced BMP-2 expression initiated bone healing via endochondral ossification. Effective transduction was additionally achieved by pre-coating micro-macroporous ceramic granules, supporting an 'off-the-shelf' approach for biomaterial-mediated tissue repair. Inducible gene delivery systems, such as the one described in this study, allow fine control of transgene expression at physiologically relevant levels, offering (i) a method to optimize growth factor delivery and release and (ii) a potential strategy for the repair of large bone defects.

Conflict of interest

Guy Daculsi is the scientific advisor of MBBCP® manufacturer, Biomatlante SA France.

Acknowledgements

This study was funded by the AO Foundation and the EU under the FP7 framework (projects GAMBIA NMP3-SL-2010-245993 and BIODESIGN NMP- 2010_LARGE-4). Computational simulations were performed at the Swiss National Supercomputing Centre (CSCS). We would like to thank Dalila Petta, Nora Goudsouzian, Mauro Bluvol and Christoph Sprecher for technical assistance. Special thanks to Phillip J. Holmes for assistance in developing the masking and colour threshold process used for histological bone quantification.

References

- Anton M, Wolf A, Mykhaylyk O *et al.* 2012; Optimizing adenoviral transduction of endothelial cells under flow conditions. *Pharm Res* 29(5): 1219–1231.
- Axelrad TW, Einhorn TA. 2009; Bone morphogenetic proteins in orthopaedic surgery. *Cytokine Growth Factor Rev* 20(5-6): 481–488.
- Bahney CS, Hu DP, Taylor AJ *et al.* 2014; Stem cell-derived endochondral cartilage stimulates bone healing by tissue transformation. *J Bone Miner Res* 29(5): 1269–1282.
- Baltzer AW, Lattermann C, Whalen JD *et al.* 2000; Genetic enhancement of fracture repair: healing of an experimental segmental defect by adenoviral transfer of the BMP-2 gene. *Gene Ther* 7(9): 734–739.
- Baltzer AW, Whalen JD, Stefanovic-Racic M *et al.* 1999; Adenoviral transduction of human osteoblastic cell cultures: a new perspective for gene therapy of bone diseases. *Acta Orthop Scand* 70(5): 419–424.
- Barradas AM, Yuan H, van Blitterswijk CA *et al.* 2011; Osteoinductive biomaterials: current knowledge of properties, experimental models and biological mechanisms. *Eur Cell Mater* 21: 407–429; discussion 429.
- Betz OB, Betz VM, Nazarian A *et al.* 2006; Direct percutaneous gene delivery to enhance healing of segmental bone defects. *J Bone Joint Surg Am* 88(2): 355–365.
- Bianchi G, Banfi A, Mastrogiacomo M *et al.* 2003; Ex vivo enrichment of mesenchymal cell progenitors by fibroblast growth factor 2. *Exp Cell Res* 287(1): 98–105.
- Breen A, Dockery P, O'Brien T *et al.* 2009; Fibrin scaffold promotes adenoviral gene transfer and controlled vector delivery. *J Biomed Mater Res A* 89(4): 876–884.
- Burchardt H. 1987; Biology of bone transplantation. *Orthop Clin North Am* 18(2): 187–196.
- Carragee EJ, Hurwitz EL, Weiner BK. 2011; A critical review of recombinant human bone morphogenetic protein-2 trials in spinal surgery: emerging safety concerns and lessons learned. *Spine J* 11(6): 471–491.
- Carreon LY, Glassman SD, Djurasovic M *et al.* 2009; RhBMP-2 versus iliac crest bone graft for lumbar spine fusion in patients over 60 years of age: a cost-utility study. *Spine* 34(3): 238–243.
- Cawthorne C, Swindell R, Stratford IJ *et al.* 2007; Comparison of doxycycline delivery methods for Tet-inducible gene expression in a subcutaneous xenograft model. *J Biomol Tech* 18(2): 120–123.
- Cho TJ, Gerstenfeld LC, Einhorn TA. 2002; Differential temporal expression of members of the transforming growth factor beta superfamily during murine fracture healing. *J Bone Miner Res* 17(3): 513–520.
- Deckers MM, van Bezooijen RL, van der Horst G *et al.* 2002; Bone morphogenetic proteins stimulate angiogenesis through osteoblast-derived vascular endothelial growth factor A. *Endocrinology* 143(4): 1545–1553.
- Egermann M, Baltzer AW, Adamaszek S *et al.* 2006; Direct adenoviral transfer of bone morphogenetic protein-2 cDNA enhances fracture healing in osteoporotic sheep. *Hum Gene Ther* 17(5): 507–517.
- Evans CH. 2012; Gene delivery to bone. *Adv Drug Deliv Rev* 64(12): 1331–1340.
- Fiorellini JP, Howell TH, Cochran D *et al.* 2005; Randomized study evaluating recombinant human bone morphogenetic protein-2 for extraction socket augmentation. *J Periodontol* 76(4): 605–613.

- Goel A, Sangwan SS, Siwach RC et al. 2005; Percutaneous bone marrow grafting for the treatment of tibial non-union. *Injury* **36**(1): 203–206.
- Gossen M, Freundlieb S, Bender G et al. 1995; Transcriptional activation by tetracyclines in mammalian cells. *Science* **268**(5218): 1766–1769.
- Goyenvalle E, Aguado E, Pilet P et al. 2010; Biofunctionality of MBCP ceramic granules (TricOs) plus fibrin sealant (Tisseel) versus MBCP ceramic granules as a filler of large periprosthetic bone defects: an investigative ovine study. *J Mater Sci Mater Med* **21**(6): 1949–1958.
- Graham FL, van der Eb AJ. 1973; A new technique for the assay of infectivity of human adenovirus 5 DNA. *Virology* **52**(2): 456–467.
- Herberg S, Kondrikova G, Hussein KA et al. 2015; Mesenchymal stem cell expression of stromal cell-derived factor-1beta augments bone formation in a model of local regenerative therapy. *J Orthop Res* **33**(2): 174–184.
- Hodges SD, Eck JC, Newton D. 2012; Retrospective study of posterior cervical fusions with rhBMP-2. *Orthopedics* **35**(6): e895–898.
- Homma Y, Zimmermann G, Hernigou P. 2013; Cellular therapies for the treatment of non-union: the past, present and future. *Injury* **44**(Suppl 1): S46–S49.
- Homminga J, Huiskes R, Van Rietbergen B et al. 2001; Introduction and evaluation of a gray-value voxel conversion technique. *J Biomech* **34**(4): 513–517.
- Horwitz EM, Gordon PL, Koo WK et al. 2002; Isolated allogeneic bone marrow-derived mesenchymal cells engraft and stimulate growth in children with osteogenesis imperfecta: implications for cell therapy of bone. *Proc Natl Acad Sci U S A* **99**(13): 8932–8937.
- Hsu WK, Sugiyama O, Park SH et al. 2007; Lentiviral-mediated BMP-2 gene transfer enhances healing of segmental femoral defects in rats. *Bone* **40**(4): 931–938.
- Hu WW, Wang Z, Hollister SJ et al. 2007; Localized viral vector delivery to enhance in situ regenerative gene therapy. *Gene Ther* **14**(11): 891–901.
- Ito H, Koefoed M, Tiyapatanaputi P et al. 2005; Remodeling of cortical bone allografts mediated by adherent rAAV-RANKL and VEGF gene therapy. *Nat Med* **11**(3): 291–297.
- Jegoux F, Goyenvalle E, Bagot D'arc M et al. 2005; In vivo biological performance of composites combining micro-macroporous biphasic calcium phosphate granules and fibrin sealant. *Arch Orthop Trauma Surg* **125**(3): 153–159.
- Jukes JM, Both SK, Leusink A et al. 2008; Endochondral bone tissue engineering using embryonic stem cells. *Proc Natl Acad Sci U S A* **105**(19): 6840–6845.
- Katayama Y, Matsuyama Y, Yoshihara H et al. 2009; Clinical and radiographic outcomes of posterolateral lumbar spine fusion in humans using recombinant human bone morphogenetic protein-2: an average five-year follow-up study. *Int Orthop* **33**(4): 1061–1067.
- Kitaori T, Ito H, Schwarz EM et al. 2009; Stromal cell-derived factor 1/CXCR4 signaling is critical for the recruitment of mesenchymal stem cells to the fracture site during skeletal repair in a mouse model. *Arthritis Rheum* **60**(3): 813–823.
- Kolar P, Schmidt-Bleek K, Schell H et al. 2010; The early fracture hematoma and its potential role in fracture healing. *Tissue Eng Part B Rev* **16**(4): 427–434.
- Kon E, Filardo G, Roffi A et al. 2012; Bone regeneration with mesenchymal stem cells. *Clin Cases Miner Bone Metab* **9**(1): 24–27.
- Kon T, Cho TJ, Aizawa T et al. 2001; Expression of osteoprotegerin, receptor activator of NF-kappaB ligand (osteoprotegerin ligand) and related proinflammatory cytokines during fracture healing. *J Bone Miner Res* **16**(6): 1004–1014.
- Konnecke I, Serra A, El Khassawna T et al. 2014; T and B cells participate in bone repair by infiltrating the fracture callus in a two-wave fashion. *Bone* **64**: 155–165.
- Kusumoto K, Bessho K, Fujimura K et al. 1998; Prefabricated muscle flap including bone induced by recombinant human bone morphogenetic protein-2: an experimental study of ectopic osteoinduction in a rat latissimus dorsi muscle flap. *Br J Plast Surg* **51**(4): 275–280.
- Le Nihouannen D, Saffarzadeh A, Gauthier O et al. 2008; Bone tissue formation in sheep muscles induced by a biphasic calcium phosphate ceramic and fibrin glue composite. *J Mater Sci Mater Med* **19**(2): 667–675.
- Lubelski D, Abdullah KG, Steinmetz MP et al. 2013; Adverse events with the use of rhBMP-2 in Thoracolumbar and lumbar spine fusions: a nine year institutional analysis. *J Spinal Disord Tech* **28**(5): E277–283.
- Luu HH, Song WX, Luo X et al. 2007; Distinct roles of bone morphogenetic proteins in osteogenic differentiation of mesenchymal stem cells. *J Orthop Res* **25**(5): 665–677.
- Marcacci M, Kon E, Moukhachev V et al. 2007; Stem cells associated with macroporous bioceramics for long bone repair: 6- to 7-year outcome of a pilot clinical study. *Tissue Eng* **13**(5): 947–955.
- Martin I, Muraglia A, Campanile G et al. 1997; Fibroblast growth factor-2 supports ex vivo expansion and maintenance of osteogenic precursors from human bone marrow. *Endocrinology* **138**(10): 4456–4462.
- Matrai J, Chuah MK, VandenDriessche T. 2010; Recent advances in lentiviral vector development and applications. *Mol Ther* **18**(3): 477–490.
- Mehrkens A, Saxer F, Guven S et al. 2012; Intraoperative engineering of osteogenic grafts combining freshly harvested, human adipose-derived cells and physiological doses of bone morphogenetic protein-2. *Eur Cell Mater* **24**: 308–319.
- Mesfin A, Buchowski JM, Zebala LP et al. 2013; High-dose rhBMP-2 for adults: major and minor complications: a study of 502 spine cases. *J Bone Joint Surg Am* **95**(17): 1546–1553.
- Moutsatsos IK, Turgeman G, Zhou S et al. 2001; Exogenously regulated stem cell-mediated gene therapy for bone regeneration. *Mol Ther* **3**(4): 449–461.
- Nasu T, Ito H, Tsutsumi R et al. 2009; Biological activation of bone-related biomaterials by recombinant adeno-associated virus vector. *J Orthop Res* **27**(9): 1162–1168.
- Neumann AJ, Schroeder J, Alini M et al. 2013; Enhanced adenovirus transduction of hMSCs using 3D hydrogel cell carriers. *Mol Biotechnol* **53**(2): 207–216.
- Nishimura R, Kato Y, Chen D et al. 1998; Smad5 and DPC4 are key molecules in mediating BMP-2-induced osteoblastic differentiation of the pluripotent mesenchymal precursor cell line C2C12. *J Biol Chem* **273**(4): 1872–1879.
- Overman JR, Farre-Guasch E, Helder MN et al. 2013; Short (15 minutes) bone morphogenetic protein-2 treatment stimulates osteogenic differentiation of human adipose stem cells seeded on calcium phosphate scaffolds in vitro. *Tissue Eng Part A* **19**(3–4): 571–581.
- Pape HC, Marcucio R, Humphrey C et al. 2010; Trauma-induced inflammation and fracture healing. *J Orthop Trauma* **24**(9): 522–525.
- Paralkar VM, Hammonds RG, Reddi AH. 1991; Identification and characterization of cellular binding proteins (receptors) for recombinant human bone morphogenetic protein 2B, an initiator of bone differentiation cascade. *Proc Natl Acad Sci U S A* **88**(8): 3397–3401.
- Pensak M, Hong S, Dukas A et al. 2015; The role of transduced bone marrow cells overexpressing BMP-2 in healing critical-sized defects in a mouse femur. *Gene Ther* **22**(6): 467–475.
- Poser L, Matthys R, Schawaldner P et al. 2014; A standardized critical size defect model in normal and osteoporotic rats to evaluate bone tissue engineered constructs. *Biomed Res Int* **2014**: 348635.
- Quarto R, Mastrogiacomo M, Cancedda R et al. 2001; Repair of large bone defects with the use of autologous bone marrow stromal cells. *N Engl J Med* **344**(5): 385–386.
- Raida M, Heymann AC, Gunther C et al. 2006; Role of bone morphogenetic protein 2 in the crosstalk between endothelial progenitor cells and mesenchymal stem cells. *Int J Mol Med* **18**(4): 735–739.
- Reddi AH, Cunningham NS. 1993; Initiation and promotion of bone differentiation by bone morphogenetic proteins. *J Bone Miner Res* **8**(Suppl. 2): S499–S502.
- Reppenhausen S, Reichert JC, Rackwitz L et al. 2012; Biphasic bone substitute and fibrin sealant for treatment of benign bone tumours and tumour-like lesions. *Int Orthop* **36**(1): 139–148.
- Ripamonti U. 1991; The induction of bone in osteogenic composites of bone matrix and porous hydroxyapatite replicas: an experimental study on the baboon (*Papio ursinus*). *J Oral Maxillofac Surg* **49**(8): 817–830.
- Ruschke K, Hiepen C, Becker J et al. 2012; BMPs are mediators in tissue crosstalk of the regenerating musculoskeletal system. *Cell Tissue Res* **347**(3): 521–544.
- Saffarzadeh A, Gauthier O, Bilban M et al. 2009; Comparison of two bone substitute biomaterials consisting of a mixture of fibrin sealant (Tisseel) and MBCP (TricOs) with an autograft in sinus lift surgery in sheep. *Clin Oral Implants Res* **20**(10): 1133–1139.
- Scotti C, Tonnarelli B, Papadimitropoulos A et al. 2010; Recapitulation of endochondral bone formation using human adult mesenchymal stem cells as a paradigm for developmental engineering. *Proc Natl Acad Sci U S A* **107**(16): 7251–7256.
- Slosar PJ, Josey R, Reynolds J. 2007; Accelerating lumbar fusions by combining rhBMP-2 with allograft bone: a prospective analysis of interbody fusion rates and clinical outcomes. *Spine J* **17**(3): 301–307.
- Solchaga LA, Penick K, Porter JD et al. 2005; FGF-2 enhances the mitotic and chondrogenic potentials of human adult bone marrow-derived mesenchymal stem cells. *J Cell Physiol* **203**(2): 398–409.
- Southwood LL, Frisbie DD, Kawcak CE et al. 2004; Evaluation of Ad-BMP-2 for enhancing fracture healing in an infected defect fracture rabbit model. *J Orthop Res* **22**(1): 66–72.
- Tirkkonen L, Haimi S, Huttunen S et al. 2013; Osteogenic medium is superior to growth factors in differentiation of human adipose stem cells towards bone-forming cells in 3D culture. *Eur Cell Mater* **25**: 144–158.
- Vogelin E, Jones NF, Huang JI et al. 2005; Healing of a critical-sized defect in the rat femur with use of a vascularized periosteal flap, a biodegradable matrix, and bone morphogenetic protein. *J Bone Joint Surg Am* **87**(6): 1323–1331.
- Wang N, Verna L, Hardy S et al. 1999; Adenovirus-mediated overexpression of c-Jun and c-Fos induces intercellular adhesion molecule-1 and monocyte chemoattractant protein-1 in human endothelial cells. *Arterioscler Thromb Vasc Biol* **19**(9): 2078–2084.
- Wang Q, Huang C, Xue M et al. 2011; Expression of endogenous BMP-2 in periosteal progenitor cells is essential for bone healing. *Bone* **48**(3): 524–532.
- Weiss P, Layrolle P, Clergeau LP et al. 2007; The safety and efficacy of an injectable bone substitute in dental sockets demonstrated in a human clinical trial. *Biomaterials* **28**(22): 3295–3305.
- Yamasaki H, Sakai H. 1992 Osteogenic response to porous hydroxyapatite ceramics under the skin of dogs. *Biomaterials* **13**(5): 308–312.
- Yang Z, Yuan H, Tong W et al. 1996. Osteogenesis in extraskeletally implanted porous calcium phosphate ceramics: variability among different kinds of animals. *Biomaterials* **17**(22): 2131–2137.
- Yoshida K, Bessho K, Fujimura K et al. 1998; Osteoinduction capability of recombinant human bone morphogenetic protein-2 in intramuscular and subcutaneous sites: an experimental study. *J Craniomaxillofac Surg* **26**(2): 112–115.
- Yuan H, Van Den Doel M, Li S et al. 2002; A comparison of the osteoinductive potential of two calcium phosphate ceramics implanted intramuscularly in goats. *J Mater Sci Mater Med* **13**(12): 1271–1275.

Supporting information

Additional Supporting Information may be found online in the supporting information tab for this article.

Figure S1. Radiograph grading score for bone defect healing as determined by two blinded, independent assessors. Grades for (i) defect tissue/material structure and (ii) bridging were combined to give a final combined radiograph score.

Figure S2. Semi-quantitation of bone formation was performed by taking (A) the total defect area and applying thresholding parameters to (B) create a mask of new callus using Adobe Photoshop CS5.